LETTERS

Gamma-secretase activating protein is a therapeutic target for Alzheimer's disease

Gen He[1], Wenjie Luo[1], Peng Li[2], Christine Remmers[1], William J. Netzer[1], Joseph Hendrick[2], Karima Bettayeb[1], Marc Flajolet[1], Fred Gorelick[3,4], Lawrence P. Wennogle[2] & Paul Greengard[1]

Accumulation of neurotoxic amyloid-β is a major hallmark of Alzheimer's disease[1]. Formation of amyloid-β is catalysed by γ-secretase, a protease with numerous substrates[2,3]. Little is known about the molecular mechanisms that confer substrate specificity on this potentially promiscuous enzyme. Knowledge of the mechanisms underlying its selectivity is critical for the development of clinically effective γ-secretase inhibitors that can reduce amyloid-β formation without impairing cleavage of other γ-secretase substrates, especially Notch, which is essential for normal biological functions[3,4]. Here we report the discovery of a novel γ-secretase activating protein (GSAP) that drastically and selectively increases amyloid-β production through a mechanism involving its interactions with both γ-secretase and its substrate, the amyloid precursor protein carboxy-terminal fragment (APP-CTF). GSAP does not interact with Notch, nor does it affect its cleavage. Recombinant GSAP stimulates amyloid-β production *in vitro*. Reducing GSAP concentrations in cell lines decreases amyloid-β concentrations. Knockdown of GSAP in a mouse model of Alzheimer's disease reduces levels of amyloid-β and plaque development. GSAP represents a type of γ-secretase regulator that directs enzyme specificity by interacting with a specific substrate. We demonstrate that imatinib, an anticancer drug previously found to inhibit amyloid-β formation without affecting Notch cleavage[5], achieves its amyloid-β-lowering effect by preventing GSAP interaction with the γ-secretase substrate, APP-CTF. Thus, GSAP can serve as an amyloid-β-lowering therapeutic target without affecting other key functions of γ-secretase.

We have reported that imatinib (also known as STI571 or Gleevec) decreases production of all amyloid-β species by inhibiting γ-cleavage of APP-CTF[5]. To identify the direct target responsible for imatinib's selective amyloid-β-lowering activity, we synthesized a photoactivatable azido imatinib derivative, G01 (Supplementary Methods and Supplementary Fig. 2). When ^{125}I-G01 was incubated with a membrane preparation followed by photolysis, none of the four components of γ-secretase were labelled. Rather, ^{125}I-G01 labelled a ~16-kDa protein (Fig. 1a, left panel) which co-immunoprecipitated with the more slowly migrating 18-kDa presenilin-1-CTF (Fig. 1a, right panel). This result was confirmed by intact-cell photolabelling using cell-permeable ^{3}H-G01: the ^{3}H-imatinib derivative did not bind to any of the four γ-secretase components, but did label a band of ~16 kDa that co-immunoprecipitated with presenilin 1 (PS1, also known as PSEN1; Fig. 1a, middle panel).

To purify the potential target protein, we synthesized a biotinylated derivative of imatinib, 'biotin-imatinib' (Supplementary Methods and Supplementary Fig. 3). Solubilized γ-secretase components, including presenilin 1, presenilin enhancer 2 and nicastrin, were specifically captured by the immobilized biotin-imatinib (Fig. 1b, left panel). A ~16-kDa band was observed by silver staining (Fig. 1b, right panel) after biotin-imatinib-bound proteins were separated by SDS–polyacrylamide gel electrophoresis, in agreement with the photolabelling results. Peptide fragments, derived from this band after trypsin digestion, and analysed by tandem mass spectrometry, corresponded to the C-terminal region of an uncharacterized protein, pigeon homologue protein (PION; human accession number, NP_059135). The identification was made on the basis of two unique tryptic peptides (^{766}LWDHPMSSNIISR^{778} and ^{779}NHVTRLLQNYKK^{790}) covering approximately 20% of the 16-kDa fragment. Its sequence, especially the C-terminal region, is highly conserved among multiple species from chicken to human (Supplementary Fig. 4). Expression pattern analysis indicates that this gene is expressed in diverse tissues, including brain (Supplementary Fig. 5). In this report, we characterize PION as a GSAP.

On the basis of its predicted sequence, the full open reading frame of human GSAP encodes a protein of 854 amino acids (~98 kDa). To determine whether the 16-kDa fragment was derived from a high-molecular-weight precursor, the metabolism of endogenous GSAP in cells was monitored by pulse–chase analysis. The results showed that GSAP is synthesized as a holoprotein (~98 kDa) and is rapidly processed into a ~16-kDa C-terminal fragment (GSAP-16K) (Fig. 1c). In the steady state, the 16-kDa fragment is the predominant form (Fig. 1c).

Incubation of cells with ^{3}H-G01, followed by photolysis and immunoprecipitation with anti-GSAP antibody, confirmed that imatinib directly binds GSAP-16K (Fig. 1d). When GSAP levels were reduced using short interfering RNA, the amount of γ-secretase (represented by PS1-CTF in Fig. 1e) associated with biotin-imatinib drastically decreased. This indicates that the affinity of imatinib for the γ-secretase complex depends on GSAP.

The effect of GSAP on amyloid-β generation is shown in Fig. 2. When siRNA was used to reduce the GSAP concentration (by 72 ± 15%) in N2a cells overexpressing APP695, the concentration of amyloid-β decreased by about 50 ± 7% (Fig. 2a); imatinib had little or no additional effect on amyloid-β concentrations. This result indicates that GSAP is the molecule through which imatinib lowers amyloid-β. GSAP knockdown resulted in decreased concentrations of all major amyloid-β species; Aβ38 by 43 ± 8%, Aβ40 by 53 ± 13% and Aβ42 by 48 ± 7% (Fig. 2b). GSAP showed no detectable effect on α- and β-cleavages (Supplementary Fig. 6). To further investigate whether GSAP can modulate γ-secretase activity, we examined the effect of purified GSAP on amyloid-β production in an *in vitro* γ-secretase assay. When recombinant GSAP-16K (amino acids 733–854 of full-length human GSAP), isolated after expression in *E. coli*, was added to membrane preparations from HEK cells containing

[1]Laboratory of Molecular and Cellular Neuroscience, The Rockefeller University, 1230 York Avenue, New York, New York 10065, USA. [2]Intra-Cellular Therapies, Inc., Audubon Biomedical Science and Technology Park, 3960 Broadway, New York, New York 10032, USA. [3]Department of Internal Medicine and Cell Biology, Yale University School of Medicine, New Haven, Connecticut 06520, USA. [4]VA Connecticut Healthcare, 333 Cedar Street, New Haven, Connecticut 06520, USA.

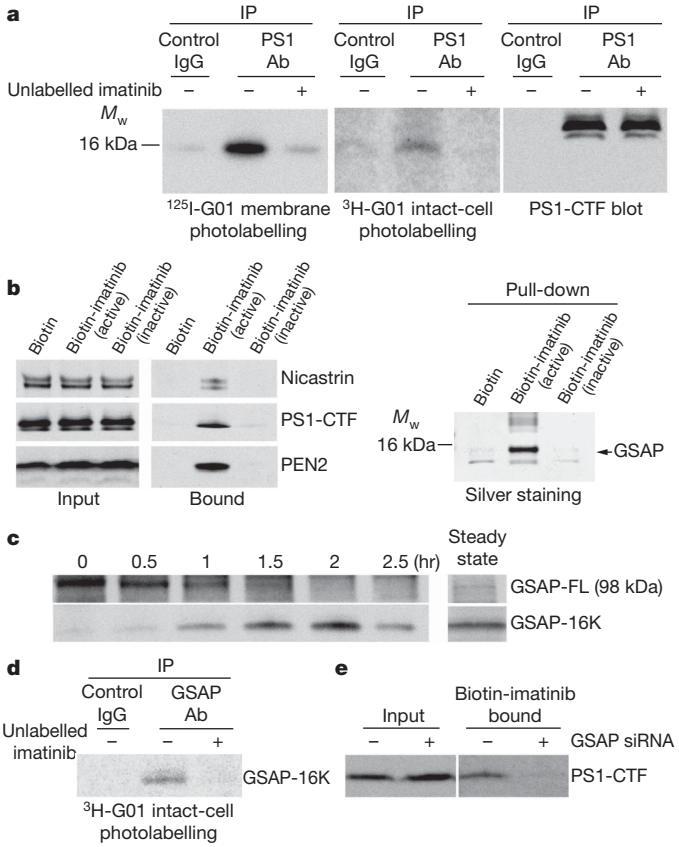

Figure 1 | Identification of GSAP as an imatinib target. **a**, A PS1-associated 16-kDa protein is labelled by a photoactivatable imatinib derivative. Left, photolysis of ^{125}I-G01 with membrane preparations. Middle, photolysis of ^{3}H-G01 with intact HEK293 cells. Right, PS1-CTF migrated with a slower mobility than the labelled 16-kDa band and was not labelled by G01. Labelling specificity was confirmed by competition with unlabelled imatinib. Ab, antibody; IgG, immunoglobulin-G; M_w, weight-averaged molecular mass. **b**, Solubilized endogenous γ-secretase components from HEK293 cells were bound to immobilized biotin-imatinib (left). Among the proteins bound to biotin-imatinib, a ~16-kDa band was detected by silver staining and was identified as the C-terminal domain of GSAP (right; arrow and label 'GSAP'). Biotin-coated beads and an inactive biotin-imatinib derivative (Supplementary Fig. 3) served as controls. PEN2, presenilin enhancer 2. **c**, Endogenous GSAP in N2a cells was synthesized as a full-length 98-kDa precursor protein (GSAP-FL) and rapidly processed into a 16-kDa C-terminal fragment. Under steady-state conditions, the predominant cellular form of GSAP was 16 kDa. **d**, Endogenous GSAP-16K was specifically labelled by ^{3}H-G01 in neuroblastoma cells. **e**, After GSAP siRNA knockdown in N2a cells, immobilized biotin-imatinib no longer captured PS1.

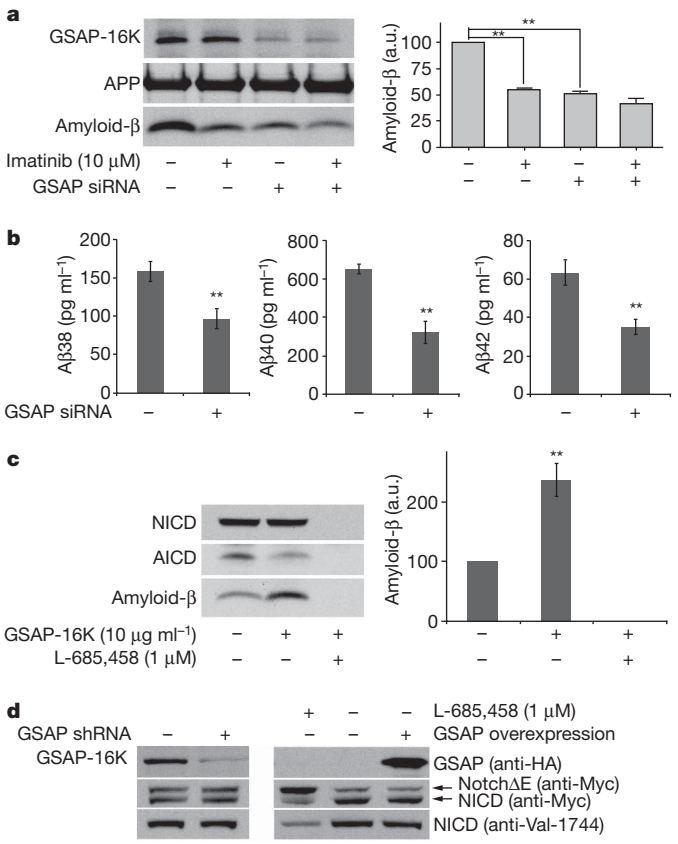

Figure 2 | GSAP regulates amyloid-β production but does not influence Notch cleavage. **a**, siRNA-mediated knockdown of GSAP in N2a cells overexpressing APP695 lowered amyloid-β production. The amyloid-β-lowering effects of imatinib and of siRNA were not additive (mean ± s.d.; $^{**}P < 0.01$; $n \geq 3$). **b**, Transfection of N2a cells overexpressing APP695 with GSAP siRNA reduced the concentrations of Aβ38, Aβ40 and Aβ42 (mean ± s.d.; $^{**}P < 0.01$; $n \geq 3$). **c**, Recombinant GSAP-16K from *E. coli* stimulated amyloid-β production in an *in vitro* γ-secretase assay, inhibited AICD production and had no effect on Notch cleavage. The γ-secretase inhibitor L-685,458 (1 μM) abolished NICD, AICD and amyloid-β production (mean ± s.d.; $^{**}P < 0.01$; $n \geq 3$). **d**, Neither GSAP knockdown (left) nor its overexpression (right) affected Notch processing in HEK293 cells overexpressing Notch without its extracellular domain (NotchΔE, with C-terminal Myc tag). NICD was detected using a Myc antibody and a cleavage-product-specific antibody (Notch1 Val-1744). The γ-secretase inhibitor L-685,458 (1 μM) served as a control. a.u., arbitrary units.

overexpressed β-secretase cleaved C-terminal fragment of APP (APP-β-CTF), the concentration of amyloid-β was increased and that of APP intracellular domain (AICD) was reduced (Fig. 2c).

APP-CTF is cleaved by γ-secretase in the middle of its transmembrane domain to generate amyloid-β (γ-cleavage) and near its cytosolic membrane boundary to generate AICD (ε-cleavage). The effect of GSAP on AICD production was examined in N2a cells overexpressing APP695. Both GSAP knockdown and imatinib treatment increased concentrations of AICD (Supplementary Fig. 7a). GSAP overexpression in HEK293 cells reduced AICD production (Supplementary Fig. 7b). These results indicate that GSAP differentially regulates γ- and ε-cleavage of APP-CTF to form amyloid-β and AICD, respectively.

One distinctive feature of imatinib is its selective inhibition of amyloid-β production while sparing Notch cleavage[5]. The effect of GSAP on Notch cleavage was evaluated using cells expressing NotchΔE (Notch without its extracellular domain), which is the Notch substrate for γ-secretase. As shown in Fig. 2d, the concentration of the γ-secretase cleavage product, the Notch intracellular domain (NICD), was not changed either by reducing GSAP concentrations using short hairpin RNA (Fig. 2d, left panel) or by overexpressing GSAP (Fig. 2d, right panel). In addition, GSAP had no effect on Notch cleavage in an *in vitro* γ-secretase assay (Fig. 2c, left panel). Thus, GSAP modulates the γ-secretase cleavage of APP but not of Notch.

Additional evidence that endogenous GSAP forms a complex with γ-secretase was provided by examining the distribution of the proteins in subcellular fractions and in co-immunoprecipitation studies. In a sucrose gradient, endogenous GSAP co-fractionated with a *trans*-Golgi network marker, and with PS1-CTF (Supplementary Fig. 8) and other γ-secretase components (not shown). Using gel filtration to separate membrane proteins from neuroblastoma cells solubilized in 1% CHAPSO, we found that endogenous GSAP-16K and γ-secretase co-migrated as a high-molecular-weight complex (Fig. 3a). Furthermore, endogenous GSAP co-immunoprecipitated with γ-secretase components, providing additional evidence that these proteins exist in a complex (Fig. 3b). Endogenous γ-secretase was isolated using an immobilized biotinylated derivative of the transition-state analogue L-685,458[6]. Endogenous GSAP-16K co-isolated with the

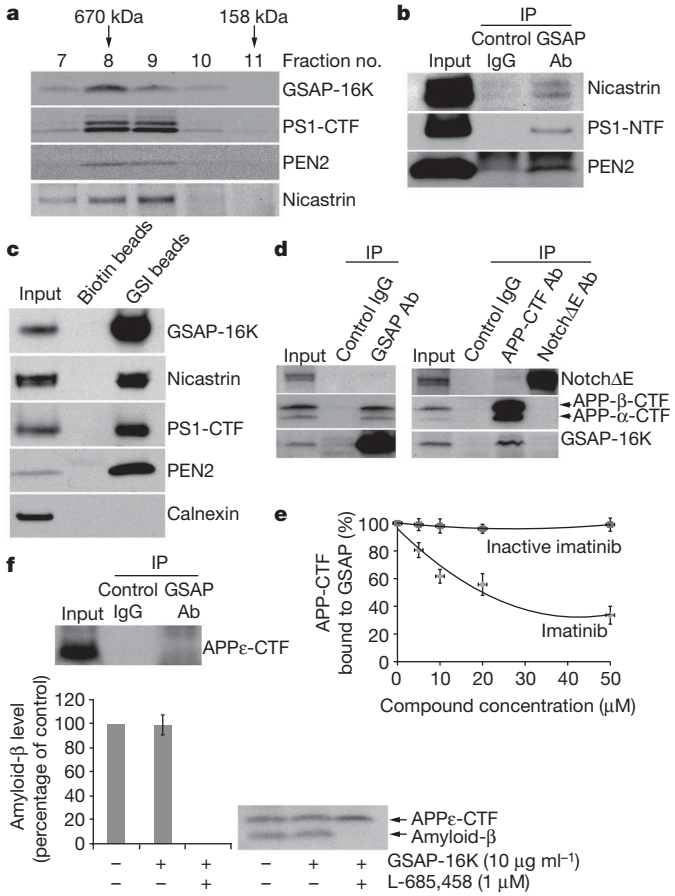

Figure 3 | GSAP interacts with γ-secretase and APP-CTF but not with Notch. **a**, Endogenous GSAP-16K in solubilized membrane preparations from N2a cells co-migrated with γ-secretase components during gel filtration (void volume: fraction 6). **b**, Immunoprecipitation of endogenous GSAP from N2a cells resulted in co-immunoprecipitation of γ-secretase components. **c**, Endogenous GSAP-16K and γ-secretase components are highly enriched by an immobilized γ-secretase transition-state analogue (GSI beads). **d**, In HEK293 cells, GSAP-16K and APP-CTF co-immunoprecipitated but NotchΔE did not. **e**, Imatinib treatment reduced the co-immunoprecipitation of APP-CTF and GSAP in a concentration-dependent manner. An inactive imatinib derivative (IC200001; see Supplementary Fig. 3) served as a negative control. **f**, In HEK293 cells, APP-CTF without the cytoplasmic domain (APPε-CTF) did not co-immunoprecipitate with GSAP-16K (top); γ-cleavage of APPε-CTF was not stimulated by GSAP-16K in an *in vitro* assay (bottom).

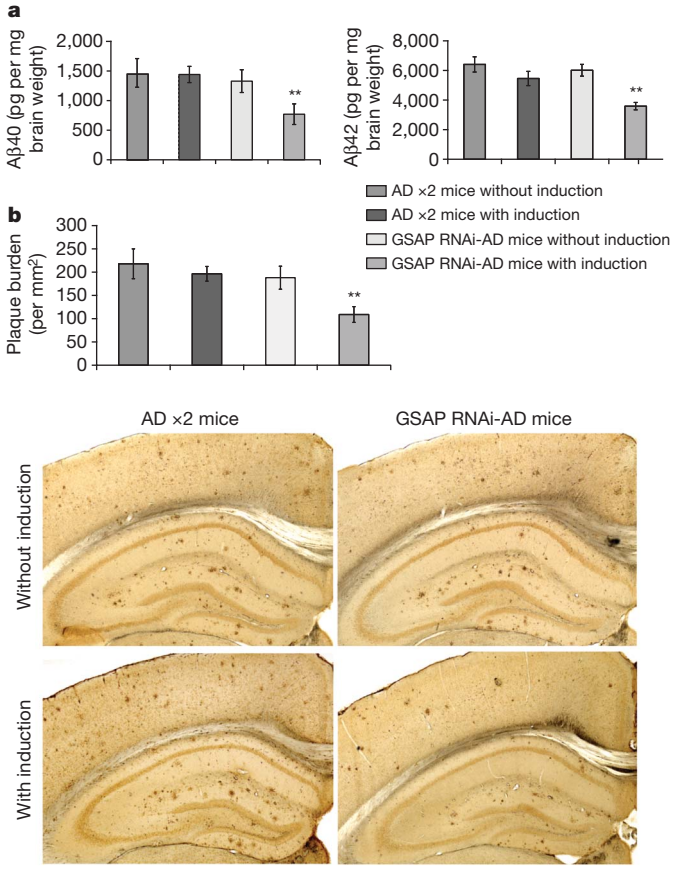

Figure 4 | Knockdown of GSAP reduces amyloid-β production and plaque development in a mouse model of Alzheimer's disease. **a**, GSAP RNAi-AD mice were generated by crossing AD ×2 mice with doxycycline-inducible GSAP RNAi mice. Six months after inducing GSAP shRNA expression, Aβ40 and Aβ42 concentrations in the crossed-mouse brains had decreased by 42 ± 13% and 40 ± 7%, respectively (mean ± s.e.m.; $^{**}P < 0.01$; $n = 4$). Doxycycline treatment alone did not change amyloid-β concentrations in AD mice. **b**, Six months after inducing GSAP shRNA expression, amyloid plaque development had reduced in the crossed-mouse brains by 38 ± 9% (mean ± s.e.m.; $^{**}P < 0.01$; $n = 4$). Doxycycline treatment alone did not change plaques in AD mice. Amyloid plaques were revealed by 6E10 immunostaining.

enzyme–inhibitor complex, strongly suggesting that GSAP-16K is a cofactor for γ-secretase (Fig. 3c).

A number of proteases with broad substrate recognition can achieve specificity through auxiliary factors that couple the core enzyme to selective substrates[7,8]. To explore the mechanism by which GSAP might confer such specificity, we analysed its association with specific substrates. GSAP-16K co-immunoprecipitated with APP-CTF but not with NotchΔE (Fig. 3d); the interaction was reduced by imatinib in a concentration-dependent manner (Fig. 3e). Disruption of this interaction by imatinib probably explains its amyloid-β-lowering activity. Domain mapping studies demonstrated that the juxtamembrane region of APP-CTF interacts with GSAP (Supplementary Fig. 9). A truncated form of APP-CTF lacking the cytoplasmic domain (APPε-CTF)[9] did not interact with GSAP and its γ-cleavage was no longer stimulated by GSAP-16K in an *in vitro* assay (Fig. 3f).

To further determine the structural basis for the selective interaction of GSAP with APP-CTF, we constructed chimaeric proteins by exchanging the AICD fragment in APP-CTF with the NICD fragment in NotchΔE (Supplementary Fig. 10a). GSAP selectively interacted with AICD but not with NICD in chimaeric proteins (Supplementary Fig. 10b). GSAP knockdown selectively increased AICD production but had no influence on NICD production from the chimaeric proteins (Supplementary Fig. 10c). These results further demonstrated that the selective effect of GSAP on APP-CTF cleavage by γ-secretase involves GSAP binding to the cytoplasmic domain of the substrate.

To determine whether our findings are relevant to Alzheimer's disease pathology, we examined the effects of GSAP on amyloid-β levels and plaque development *in vivo*. A conditional GSAP RNA interference mouse line was generated by integration of a tetracycline-inducible GSAP shRNA vector into the mouse genomic locus. GSAP RNAi mice were then crossed with a mouse model of Alzheimer's disease (APPswe and PS1ΔE9 mutations; double-transgenic Alzheimer's disease (AD ×2) mice)[10]. To examine the long-term effect of GSAP knockdown on amyloid-β concentrations and plaque development, the crossed GSAP RNAi-AD ×2 mice were continuously induced for six months. After induction, GSAP messenger RNA concentrations in these hybrid mouse brains were reduced by 85 ± 12% and similar decreases were achieved in other tissues; after six months of induction, Aβ40 and Aβ42 concentrations in the crossed mouse brains were lowered by 42 ± 13% and 40 ± 7%, respectively (Fig. 4a). Amyloid plaque load in crossed mouse brains with GSAP knockdown was reduced by 38 ± 9% relative to the same line of mouse brains without induction (Fig. 4b). Doxycycline did not have an effect

on either amyloid-β or plaque concentrations in AD ×2 mice. The amyloid-β-lowering effects of GSAP knockdown are similar to those caused by the γ-secretase inhibitor dibenzazepine[11] (DBZ), administered at 10 μmol kg^{-1} for five days (Supplementary Fig. 11a). In contrast, GSAP knockdown did not cause the intestinal mucosal cell metaplasia seen with DBZ (Supplementary Fig. 11b): the latter effect is mediated by impaired Notch processing[4,11]. Furthermore, GSAP knockdown did not cause any pathological changes in spleen (data not shown), whereas severe marginal-zone lymphoid depletion was caused by DBZ administration[12]. These results indicate that GSAP knockdown reduces amyloid-β concentrations and plaque formation without affecting Notch-dependent pathways.

Gamma-secretase processes diverse substrates with low homologies at their cleavage sites[13]. The various roles of γ-secretase during development and in tissue homeostasis require that its activity be tightly regulated. TMP21[14] (also known as TMED10), orphan G-protein-coupled receptor 3[15] and different Aph1 isoforms[16] have been reported to modulate amyloid-β production through γ-secretase but to spare Notch cleavage. However, the underlying molecular mechanisms by which they impart their specificities were not elucidated in those studies. Nevertheless, the studies demonstrated that it is possible to selectively regulate substrate specificity of this vitally important and potentially promiscuous enzyme. GSAP seems to confer substrate specificity on γ-secretase by forming a ternary complex with γ-secretase and the substrate APP-CTF. The present results support the concept that appropriate cofactors impart substrate specificity on the γ-secretase core enzyme complex, as they do on a number of other proteases[7,8].

The literature on the relationship between γ- and ε-cleavage of APP-CTF is controversial. For instance, there is some evidence supporting sequential cleavage of APP-CTF[9,17]. There is also extensive evidence reported in the literature that these two types of cleavage can occur independently[18–20]. Our data support the second hypothesis. We propose that removal of GSAP from the GSAP/γ-secretase/APP-CTF ternary complex alters the structural relationship between γ-secretase and APP-CTF, facilitating ε-cleavage at the expense of γ-cleavage (Supplementary Fig. 1). To elucidate the detailed mechanism by which GSAP modulates the cleavage of APP-CTF, it will be important to compare the stoichiometry of the various γ-secretase cleavage products in the presence and absence of GSAP.

Anti-amyloid therapy remains a rational approach to the treatment of Alzheimer's disease. One promising anti-amyloid compound failed in limited clinical trials, owing to lack of accumulation in the brain[21]. Similarly, imatinib is actively excluded from the brain by a highly potent P-glycoprotein pump, a component of the blood–brain barrier[22]. The development of compounds that accumulate in the brain and target GSAP represents a valid approach for development of potential therapies against Alzheimer's disease.

METHODS SUMMARY

See Methods for details of *in vitro* and intact-cell photolabelling, affinity purification using immobilized biotin-imatinib, GSAP knockdown and overexpression, co-immunoprecipitation, gel filtration chromatography, affinity capture of endogenous γ-secretase using an immobilized transition-state analogue, *in vitro* γ-secretase assay, GSAP RNAi mouse line generation, induction, immunohistochemistry and amyloid-β measurements.

Full Methods and any associated references are available in the online version of the paper at www.nature.com/nature.

Received 13 September 2009; accepted 5 July 2010.

1. Selkoe, D. J. Alzheimer's disease: genes, proteins, and therapy. *Physiol. Rev.* **81,** 741–766 (2001).
2. Steiner, H., Fluhrer, R. & Haass, C. Intramembrane proteolysis by gamma-secretase. *J. Biol. Chem.* **283,** 29627–29631 (2008).
3. Lathia, J. D., Mattson, M. P. & Cheng, A. Notch: from neural development to neurological disorders. *J. Neurochem.* **107,** 1471–1481 (2008).
4. Wong, G. T. *et al.* Chronic treatment with the gamma-secretase inhibitor LY-411,575 inhibits beta-amyloid peptide production and alters lymphopoiesis and intestinal cell differentiation. *J. Biol. Chem.* **279,** 12876–12882 (2004).
5. Netzer, W. J. *et al.* Gleevec inhibits beta-amyloid production but not Notch cleavage. *Proc. Natl Acad. Sci. USA* **100,** 12444–12449 (2003).
6. Placanica, L. *et al.* Pen2 and presenilin-1 modulate the dynamic equilibrium of presenilin-1 and presenilin-2 gamma-secretase complexes. *J. Biol. Chem.* **284,** 2967–2977 (2009).
7. Dougan, D. A., Mogk, A., Zeth, K., Turgay, K. & Bukau, B. AAA+ proteins and substrate recognition, it all depends on their partner in crime. *FEBS Lett.* **529,** 6–10 (2002).
8. Visintin, R., Prinz, S. & Amon, A. CDC20 and CDH1: a family of substrate-specific activators of APC-dependent proteolysis. *Science* **278,** 460–463 (1997).
9. Lefranc-Jullien, S., Sunyach, C. & Checler, F. APPε, the ε-secretase-derived N-terminal product of the β-amyloid precursor protein, behaves as a type I protein and undergoes α-, β-, and γ-secretase cleavages. *J. Neurochem.* **97,** 807–817 (2006).
10. Jankowsky, J. L. *et al.* Co-expression of multiple transgenes in mouse CNS: a comparison of strategies. *Biomol. Eng.* **17,** 157–165 (2001).
11. van Es, J. H. *et al.* Notch/gamma-secretase inhibition turns proliferative cells in intestinal crypts and adenomas into goblet cells. *Nature* **435,** 959–963 (2005).
12. Milano, J. *et al.* Modulation of notch processing by gamma-secretase inhibitors causes intestinal goblet cell metaplasia and induction of genes known to specify gut secretory lineage differentiation. *Toxicol. Sci.* **82,** 341–358 (2004).
13. Beel, A. J. & Sanders, C. R. Substrate specificity of gamma-secretase and other intramembrane proteases. *Cell. Mol. Life Sci.* **65,** 1311–1334 (2008).
14. Chen, F. *et al.* TMP21 is a presenilin complex component that modulates gamma-secretase but not epsilon-secretase activity. *Nature* **440,** 1208–1212 (2006).
15. Thathiah, A. *et al.* The orphan G protein-coupled receptor 3 modulates amyloid-beta peptide generation in neurons. *Science* **323,** 946–951 (2009).
16. Serneels, L. *et al.* γ-secretase heterogeneity in the Aph1 subunit: relevance for Alzheimer's disease. *Science* **324,** 639–642 (2009).
17. Takami, M. *et al.* γ-secretase: successive tripeptide and tetrapeptide release from the transmembrane domain of beta-carboxyl terminal fragment. *J. Neurosci.* **29,** 13042–13052 (2009).
18. Kume, H. & Kametani, F. Abeta 11–40/42 production without gamma-secretase epsilon-site cleavage. *Biochem. Biophys. Res. Commun.* **349,** 1356–1360 (2006).
19. Wiley, J. C., Hudson, M., Kanning, K. C., Schecterson, L. C. & Bothwell, M. Familial Alzheimer's disease mutations inhibit gamma-secretase-mediated liberation of beta-amyloid precursor protein carboxy-terminal fragment. *J. Neurochem.* **94,** 1189–1201 (2005).
20. Bentahir, M. *et al.* Presenilin clinical mutations can affect gamma-secretase activity by different mechanisms. *J. Neurochem.* **96,** 732–742 (2006).
21. Green, R. C. *et al.* Effect of tarenflurbil on cognitive decline and activities of daily living in patients with mild Alzheimer disease: a randomized controlled trial. *J. Am. Med. Assoc.* **302,** 2557–2564 (2009).
22. Dai, H., Marbach, P., Lemaire, M., Hayes, M. & Elmquist, W. F. Distribution of STI-571 to the brain is limited by P-glycoprotein-mediated efflux. *J. Pharmacol. Exp. Ther.* **304,** 1085–1092 (2003).

Supplementary Information is linked to the online version of the paper at www.nature.com/nature.

Acknowledgements We thank E. Woo and B. Chait for their help with protein identification. We thank Y. M. Li for providing us with the biotinylated transition-state analogue. We thank B. Turner and S. Ku for their technical support. This work was supported by NIH grant AG09464 to P.G., DOD grant W81XWH-09-1-0402 to P.G., the Fisher Center for Alzheimer's Research Foundation and the F. M. Kirby Foundation.

Author Contributions G.H., W.L., P.L., C.R., J.H. and K.B. performed experiments; W.J.N. was involved in experimental design; M.F. performed sequence analysis; G.H., W.L., L.P.W. and P.G. designed the study; G.H., W.L., F.G., L.P.W. and P.G. wrote the paper; all authors discussed the results and commented on the manuscript.

Author Information Reprints and permissions information is available at www.nature.com/reprints. The authors declare competing financial interests: details accompany the full-text HTML version of the paper at www.nature.com/nature. Readers are welcome to comment on the online version of this article at www.nature.com/nature. Correspondence and requests for materials should be addressed to P.G. (greengard@rockefeller.edu).

METHODS

***In vitro* and intact-cell photolabelling.** For *in vitro* labelling, resuspended membranes isolated from HEK293 cells were incubated with 20 nM ^{125}I-G01 for 3 h at 4 °C before photolysis at 254 nM for 2 min. For intact-cell labelling, HEK293 cells were incubated with 0.1 μM ^{3}H-G01 in Opti-MEM for 2 h at 37 °C before being transferred to ice for an additional hour. To examine labelling specificity, either membrane preparations or cells were treated with 50 μM unlabelled imatinib together with photoactivatable G01 in parallel assays. Photolysis was conducted on ice for 2 min at 254 nm. After photolysis, membranes or cells were disrupted in lysis buffer (50 mM HEPES, 150 mM NaCl, 1% CHAPSO with protease inhibitors) and immunoprecipitated with PS1-loop antibody. The immunopurified material was eluted with SDS sample buffer and proteins were separated using a 10–20% Tris-tricine SDS–PAGE gel and transferred to PVDF for autoradiography.

Affinity purification using immobilized biotin-imatinib. Membrane preparations of HEK293 cells were solubilized in lysis buffer (50 mM HEPES, 150 mM NaCl, 5 mM $MgCl_2$, 5 mM $CaCl_2$ and 1% CHAPSO containing protease inhibitors; Roche) and incubated with MyOne streptavidin T1 beads (Invitrogen) containing bound biotin-imatinib for 3 h at 4 °C. Subsequently, the beads were washed three times with lysis buffer. Bound proteins were eluted with tricine SDS–PAGE sample buffer and separated on 10–20% Tris-tricine gels. Silver staining was used to identify protein bands in SDS–PAGE gels. The ~16-kDa band was excised, trypsinized and sequenced by tandem MS/MS mass spectrometry.

GSAP antibody production and metabolic labelling. Rabbit polyclonal antiserum against GSAP was generated against the peptide CFEGHDNVDAEFV EEAALKHT (corresponding to amino acids 829–848 of human GSAP with an amino-terminal cysteine attached for conjugation). Pulse–chase labelling experiments using neuroblastoma 2a (N2a) cells were conducted as described previously[23]. Cells were pulsed for 15 min, the chase periods were initiated by replacing the medium with full culture medium and cells were incubated at 37 °C. For continuous labelling, cells were labelled with ^{35}S Protein Labelling Mix (Perkin Elmer) for 4 h without chase. Cell monolayers were lysed in RIPA buffer followed by immunoprecipitation with GSAP antibody. The beads were incubated with Tris-tricine sample buffer to elute bound proteins, which were then separated by 10–20% Tris-tricine gel and transferred to PVDF membrane for autoradiography.

Cellular knockdown and overexpression. For cellular GSAP knockdown experiments, siRNA of GSAP was purchased from Dharmacon. The sequences of the siRNA used were as follows: sense sequence, 5′-AUGCAGAGCUGGACG ACAUUU-3′; antisense sequence, 5′-PAUGUCGUCCAGCUCUGCAUUU-3′. An N2a cell line stably overexpressing APP695 was transfected with siRNA using DharmaFect 2 reagent at a concentration of 50 nM. Non-targeting control siRNA (Dharmacon) was transfected in parallel as control. shRNA of GSAP was purchased from Open Biosystems and transfected into cells using Arrest-In transfection reagent (Open Biosystems). The sequence of human GSAP shRNA in pGIPZ shRNAmir-GFP vector was as follows: TGCTGTTGACAGTG AGCGCGGAAATAGAGTGGTGATTAAATAGTGAAGCCACAGATGTATTT AATCACCACTCTATTTCCATGCCTACTGCCTCGGA. The knockdown efficiencies were examined using a real-time PCR assay with an Applied Biosystems 7900 HT System.

For GSAP overexpression in cells, mammalian expression vector pReceiver-M07 with the full-length GSAP coding a C-terminal HA tag was purchased from Genecopoeia. Plasmid was transfected into a stable HEK293 cell line overexpressing APP695, containing the Swedish mutation, using Lipofectamine 2000 (Invitrogen). pcDNA4-APP-β-CTF expression vector was a kind gift from Dr. Y. M. Li (Memorial Sloan Kettering Cancer Center). APPε-CTF construct was derived from the pcDNA4-APP-β-CTF as reported previously[9].

The concentrations of amyloid-β species were quantified using a highly sensitive ECL assay from Meso Scale Drug Discoveries. Immunoprecipitation of amyloid-β was performed as described prevously[5].

For Notch cleavage analysis, cells transfected with NotchΔE[5] were co-transfected with GSAP-shRNA or GSAP plasmids. After two days of transfection, Notch expression and cleavage were detected with anti-Myc antibody. The cleaved Notch intracellular domain (NICD) was detected with a cleavage-specific antibody (Notch1 Val-1744, Cell Signaling). Cells treated with L-685,458 served as controls.

Co-immunoprecipitation. For co-immunoprecipitation, cells were lysed in 50 mM HEPES, 150 mM NaCl, 5 mM $MgCl_2$, 5 mM $CaCl_2$ and 1% CHAPSO, with protease inhibitors. Immunoprecipitation was performed using the corresponding antibody and protein G plus/protein A beads for 2 h on ice. Immunoprecipitated proteins were resolved by SDS–PAGE and analysed by immunoblots. Presenilin 1 loop antibody (EMD Biosciences) was used to detect PS1-CTF; PEN2 antibody was purchased from EMD Biosciences. Nicastrin antibody was from BD Biosciences. HA monoclonal antibody and Myc tag polyclonal antibody were from Genscript. APP-CTF was detected using the 369 antibody[24]. 6E10 and 4G8 antibodies from Covance were used to detect amyloid-β.

Gel filtration chromatography. Solubilized membrane preparations from N2a cells (0.2 ml, ~1 mg of solubilized protein, in 50 mM HEPES, 150 mM NaCl, 1% CHAPSO, 5 mM $MgCl_2$, 5 mM $CaCl_2$) were applied to a Superdex 200 10/300 GL column (GE Healthcare) of an AKTA fast performance liquid chromatography system. Fractionation was performed in the lysate buffer at a flow rate of 0.5 ml min^{-1} and 1-ml fractions were collected. Endogenous GSAP was detected after immunoprecipitated with GSAP antibody. Each fraction was analysed by immunoblot using γ-secretase antibodies.

Affinity capture of endogenous γ-secretase using an immobilized transition-state analogue. Compound 4, a biotinylated γ-secretase transition-state analogue[6], was a kind gift from Dr. Y. M. Li. HEK293 cell lysates in 50 mM HEPES, 150 mM NaCl, 1% CHAPSO, 5 mM $MgCl_2$ and 5 mM $CaCl_2$ were incubated with compound 4 immobilized on MyOne streptavidin magnetic beads for 2 h at 4 °C. The beads were then washed three times with lysate buffer. The captured proteins were eluted with SDS sample buffer, separated by SDS–PAGE and processed for immunoblot analysis.

***In vitro* γ-secretase assay.** The *in vitro* γ-secretase assay was based on that described previously[25] except for the use of APP-CTF or NotchΔE overexpressed in HEK293 cells rather than recombinant proteins from *E. coli*. Recombinant GSAP-16K (amino acids 733–854 of the human GSAP) was expressed in BL21 DE3 *E. coli* and purified. After 2 h of ^{35}S labelling, membrane preparations from HEK293 cells overexpressing APP-CTF were resuspended in 200 μl of assay buffer with 2 μg recombinant GSAP-16K or the same amount of BSA as control. A parallel system with 1 μM L-685,458 (γ-secretase inhibitor) was also used as a control. The membrane suspension was pre-incubated at 4 °C for 1 h and then incubated for 2 h at 37 °C to allow *in vitro* generation of amyloid-β. Amyloid-β was immunoprecipitated from the lysate using 4G8 antibody, separated on 10–20% Tris-tricine gel and transferred to PVDF membrane for autoradiography.

GSAP RNAi mouse line generation. Inducible RNAi mice were generated by incorporating GSAP shRNA 5′-TCCCGGAACTCCATGATTGACAAATTTC AAGAGAATTTGTCAATCATGGAGTTCCTTTTTA-3′ into the mouse genome (B6/129S6 background) under the control of a H1-Tet promoter, as described previously[26] (TaconicArtemis). Heterozygous RNAi mice were then crossed with an Alzheimer's disease mouse model with APPswe and PS1Δ9 mutations (AD ×2 mice) to generate GSAP-RNAi AD mice for amyloid-β analyses.

Induction of GSAP RNAi-AD mouse, measurement of amyloid-β concentration and histochemical analysis. shRNA was induced in two-month-old GSAP RNAi-AD mice with doxycycline for one month by adding 2 mg ml^{-1} doxycycline (Sigma) into drinking water containing 10% sucrose. Control mice were fed drinking water containing 10% sucrose. GSAP knockdown efficiency in mice was assayed using real-time PCR. Amyloid-β concentrations from mouse hippocampus were measured by ELISA (Wako Chemicals). Intestinal dissection and histochemical staining (H&E and PAS staining) were conducted as described elsewhere[11].

For immunohistochemistry studies, mouse brains were processed and labelled with the anti-amyloid-β antibody 6E10 (Novus Biologicals) to visualize extracellular amyloid plaques using an MOM immunodetection kit (Vector Laboratories).

23. Wang, H. *et al.* Presenilins and gamma-secretase inhibitors affect intracellular trafficking and cell surface localization of the gamma-secretase complex components. *J. Biol. Chem.* **279**, 40560–40566 (2004).
24. Xu, H. *et al.* Estrogen reduces neuronal generation of Alzheimer beta-amyloid peptides. *Nature Med.* **4**, 447–451 (1998).
25. Li, Y. M. *et al.* Presenilin 1 is linked with gamma-secretase activity in the detergent solubilized state. *Proc. Natl Acad. Sci. USA* **97**, 6138–6143 (2000).
26. Seibler, J. *et al.* Reversible gene knockdown in mice using a tight, inducible shRNA expression system. *Nucleic Acids Res.* **35**, e54 (2007).